Structure and optical absorption of combustion-synthesized nanocrystalline $LiCoO_2$

Paromita Ghosh, S. Mahanty, M.W. Raja, R.N. Basu,[a] and H.S. Maiti
Fuel Cell and Battery Section, Electroceramics Division, Central Glass and Ceramic Research Institute, Kolkata 700 032, India

(Received 7 March 2006; accepted 3 August 2006)

Nanocrystalline $LiCoO_2$ powders (10–50 nm) were synthesized by a citrate-nitrate combustion process followed by calcination at different temperatures (300–800 °C) in air. Thermogravimetric analyses indicated a sharp combustion at a low temperature of 225 °C, producing fine crystallites. Quantitative phase analyses from the x-ray diffractograms showed that while annealing at 500 °C produced mixed phases of cubic and rhombohedral $LiCoO_2$, annealing at 800 °C resulted in single-phase rhombohedral $LiCoO_2$. Electronic transitions related to the Co 3*d* bands were investigated by ultraviolet-visible reflectance spectra in absorbance mode and were ascribed to the Co 3*d* intra-band transition involving t_{2g} and e_g orbitals. The *d-d* transitions underwent a blue shift of about 0.3 eV as the cubic $LiCoO_2$ transformed into the rhombohedral structure with band gap values of about 1.4 and 1.7 eV.

I. INTRODUCTION

In recent years, extensive research has been focused on $LiCoO_2$ for cathode materials in lithium ion secondary batteries because it possesses a high cell voltage of about 4 V, high charge capacity of around 120 $mAhg^{-1}$, a long cycle life, and a low self discharge.[1–3] Understanding the electronic structure and the electronic processes involved in Co 3*d* bands in $LiCoO_2$ is a very crucial issue as most of its electrochemical properties would be affected by the electronic structure. Depending upon the temperature, $LiCoO_2$ exists in two crystalline forms: a low-temperature (LT) (<500 °C) cubic spinel (space group $Fd3m$) and a high-temperature (HT) (>500 °C) layered rock-salt structure (space group $R\bar{3}m$), commonly known as LT and HT $LiCoO_2$, respectively, in the literature.[4–12] Both structures are based on the same oxide sublattice (a cubic close-packed oxygen network) but differ essentially in the spatial arrangement of the cations. The cubic phase of $LiCoO_2$ is characterized by a random distribution of cobalt and lithium cation layers of about 75% Co and 25% Li (Co-rich layer) alternating with cation layers of about 25% Co and 75% lithium (Li-rich layer) whereas the rhombohedral phase is distinguished by an ideal rocksalt α-sodium ferrite (α–$NaFeO_2$) structure showing alternating layers of Li and Co.[12] The layered rock-salt form of $LiCoO_2$ consists of slightly distorted CoO_6 octahedra; thus a ligand field is strong enough to stabilize a Co^{3+} low-spin ground state, and hence, all six 3*d* electrons of Co^{3+} have a low-spin configuration.[13,14] Co 3*d* bands of layered rock-salt $LiCoO_2$ consist of three t_{2g} (valence band) and two e_g (conduction band) levels. The crystal structure of Co_3O_4 represents a normal spinel structure with Co^{2+} ions occupying tetrahedral sites with lower e_g and higher t_{2g} orbitals and Co^{3+} ions occupying octahedral sites with lower t_{2g} and higher e_g orbitals in the ligand field of oxygen ions.[4,8] Although, like Co_3O_4, cubic $LiCoO_2$ has a normal spinel structure, recent studies by Shao-Horn et al.[15] using electron diffraction show that the cation distribution is different in $LiCoO_2$ such that only Co^{3+} ions are present in the octahedral sites, though the possibility of some minute Co^{2+} defects residing in the tetrahedral sites cannot be completely ruled out. Therefore, while the conduction band in the case of Co_3O_4 is formed by the hybridization of four empty e_g (Co^{3+}) and three t_{2g} holes (Co^{2+}),[16] the conduction band of cubic $LiCoO_2$ is formed by the four empty e_g holes alone. Aydinol et al.[13] found a value of ~2.2 eV for the t_{2g}–e_g separation from the band-structure calculations of $LiCoO_2$ using the ab initio pseudopotential method and ascribed it to a downshift of the e_g density of states in comparison to CoO (~2.3 eV) due to an increase in Co–O bond length resulting from Li incorporation into CoO. On the other hand, Czyzyk et al.[14] performed the calculations by the localized spherical wave (LSW) method and predicted a value of 1.7 eV. Elp et al.[16] investigated the electronic structure of $LiCoO_2$ by x-ray photo electron spectroscopy (XPS) and Bremsstrahlung isochromat spectroscopy (BIS) and reported a band gap of 2.7 eV. After a few years, Rosolen et al.[17]

[a]Address all correspondence to this author.
e-mail: rnbasu@cgcri.res.in
DOI: 10.1557/JMR.2007.0157

observed that the Co–O bond length increases from 1.905 to 1.933 Å for $Li_{0.5}CoO_2$ to $LiCoO_2$, and from the photocurrent spectra studies, the authors estimated a band gap of 2.5 eV. These studies show a considerable spread in the band gap value of $LiCoO_2$, both in theoretical calculations and in experimental results (1.7–2.5 eV).

Recently, Kushida et al.[5,18] used ultraviolet-visible (UV-vis) spectroscopy to study the electronic transitions in layered rhombohedral $LiCoO_2$ by depositing thin films onto Si or SiO_2 substrates. They observed a prominent absorption peak at ~2.1 eV, which was attributed to the *d-d* transition. However, polycrystalline thin films always show a higher band gap value compared to the bulk powder or single-crystal materials. Moreover, as the actual electrodes are made out of bulk powder, it seems necessary to experimentally investigate the *d-d* transition processes in bulk $LiCoO_2$ in more detail both in the rhombohedral and the cubic form. Hence, with this objective in mind, in the present work, the phase transformation and the associated optical transitions in each phase were studied systematically for combustion-synthesized $LiCoO_2$ powder samples.

II. EXPERIMENTAL

$LiCoO_2$ powders were synthesized through a conventional citrate-nitrate gel combustion process.[19] An aqueous solution of lithium nitrate ($LiNO_3$), cobaltous nitrate hexahydrate [$Co(NO_3)_2.6H_2O$] (s.d. fine Chemicals, India, 99.5%) and citric acid monohydrate (Merck, India, 99.0%) was heated on a hot plate at a temperature of ~150 °C. Citric acid was added in required quantities to control the citrate-to-nitrate (C/N) ratio. Citric acid acted both as a fuel for the combustion process as well as a chelating agent for the metal ions (Li^+ and Co^{++}) in solution. The homogeneity of the solution was ensured by constant stirring of the solution by a magnetic needle. The heating was continued until the clear dark purple solution turned into a viscous gel and ultimately burned into a black mass containing the precursor metal oxides for the formation of $LiCoO_2$. The as-synthesized $LiCoO_2$ powder was collected and subjected to further heat treatment in air at three different temperatures, 300, 500, and 800 °C, for a period of 5 h. These three samples are henceforth referred to as C3, C5, and C8, respectively, and the as-synthesized powder is referred to as C.

Thermogravimetric analyses (TGA) of the gel and the as-synthesized powder sample were performed in the temperature ranges 30–600 °C and 30–1000 °C, respectively, by a Shimadzu Thermal Analyzer (Model TA-50, Japan) with a heating rate of 10 °C/min. X–ray powder diffractograms were recorded in the 2θ range 15–70° at a scanning rate of 2°/min by a Philips X'Pert x-ray diffractometer (The Netherlands) with Cu K_α radiation at 40 KV and 40 mA. A slow scanning at a rate of 0.4°/min in the 2θ range 55–75° was performed to allow clear observation of the splitting of the higher angle peaks characteristic of the rhombohedral phase. Rietveld refinement of the powder x-ray diffraction (XRD) profiles and quantitative phase analysis were carried out with the PANalytical Highscore Plus Program (PANanalytical B.V., The Netherlands). The size–strain analysis was performed by comparing the XRD peak profile width to that of a standard silicon scan to account for the instrumental broadening. Fourier transform infrared spectroscopy (FTIR) was carried out in the wave number range of 2500–400 cm^{-1} by a Nicolet 5 PC spectrometer (Thermo Fisher Scientific, Inc., US). The morphology of the samples was examined by a ZEISS Supra 35 (Germany) field emission scanning electron microscope (FE-SEM). Optical reflectance spectra in the absorbance mode of the samples were recorded in the wavelength range of 200–2000 nm using a Shimadzu UV3100 UV-vis spectrophotometer (Japan). For comparison, absorption spectrum for Co_3O_4 was also recorded in the same wavelength range. Inductively coupled plasma (ICP) analyses of the $LiCoO_2$ samples were performed with a Spectro Flame ICP-AES Spectrometer (Germany).

III. RESULTS AND DISCUSSION

Figure 1(a) shows the TGA plot of the gel. An initial weight loss was observed below 150 °C, which is due to the removal of the absorbed water.[20] At around 225 °C, a sharp weight loss of about 93% was observed, indicating instantaneous combustion, and could be related to the formation of $LiCoO_2$. It was confirmed by quantitative phase analyses of the as-synthesized powder (sample C) that a considerable amount of CoO was present as a second phase along with $LiCoO_2$ in this sample. Among the oxides of cobalt, CoO is formed at temperatures above 800 °C.[20] Thus, the presence of CoO in the as-synthesized powder indicated that during combustion the flame temperature exceeded 800 °C. After 225 °C, except for a small weight gain of about 2% at ~280 °C, no

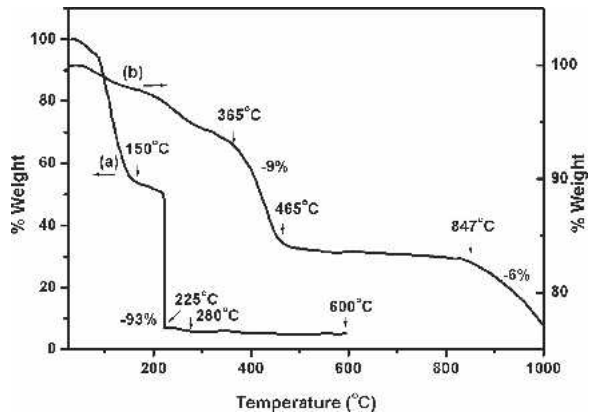

FIG. 1. TGA curves for (a) precursor gel and (b) as-synthesized $LiCoO_2$.

TABLE I. Structural and optical results for the synthesized nanocrystalline $LiCoO_2$.

Sample code	Calcination temperature (°C; time = 5 h)	Phases				Lattice parameters of $LiCoO_2$ (Å)		Crystallite size of $LiCoO_2$ (nm)	Band gap of $LiCoO_2$ phase (eV)
		$LiCoO_2$ (C)	Co_3O_4 (C)	CoO (C)	$LiCoO_2$ (R)	*a* (±0.0002)	*c* (±0.0002)		
C	As-synthesized	46%	⋯	54%	⋯	8.0230	⋯	⋯	⋯
C3	300	46%	54%	⋯	⋯	7.9831	⋯	10	1.43
C5	500	15%	⋯	⋯	85%	2.8174	14.0229	19	1.69
C8	800	⋯	⋯	⋯	100%	2.8141	14.0433	51	1.68

further significant change in weight was observed up to 600 °C. This small weight gain may have been caused by the conversion of CoO to the low-temperature stable form, Co_3O_4, on heating.[21] Figure 1(b) shows the TGA curve of the as-synthesized powder (sample C). The curve consists of four segments: below 365 °C, a gradual weight loss was observed, which may have been caused by the removal of absorbed moisture and organic moieties. Between 365 and 465 °C, about 9% of the weight loss occurred. If this is considered along with the XRD results (Table I), the weight loss was probably caused by the conversion of Co_3O_4 to $LiCoO_2$. This was followed by a plateau region up to 850 °C and thereafter, a weight loss of about 6% took place up to 1000 °C, caused by lithium evaporation.[20] Figures 2(a) and 2(b) show the XRD lines corresponding to JCPDS data files 82-0330 and 50-0653 for cubic and rhombohedral $LiCoO_2$, respectively. Figures 2(c-i)–2(c-iv) show the x-ray diffractograms for the as-synthesized (sample C) and the heat-treated samples (C3, C5 and C8) with the *hkl* values given in parentheses. The diffractogram of sample C [Fig. 2(c-i)] is marked by several broad peaks suggesting a smaller crystallite size and/or poor crystallinity. All the peaks were identified with a cubic spinel phase of $LiCoO_2$ along with cubic CoO. The peaks at $2\theta = 42.7$ and $2\theta = 69.54$, marked with asterisks [Fig 2(c-i)], are the 100% and 50% peaks of CoO.[22] The diffractogram for sample C3 [Fig. 2(c-ii)] shows the peak with *hkl* (311) at $2\theta = 37.08$ as the most intense peak, characteristic of cubic $LiCoO_2$, and the other notable peaks are those with *hkl* (111) at $2\theta = 19.08$, (220) at $2\theta = 31.42$, and (440) at $2\theta = 65.46$. The peak with *hkl* (531) at $2\theta = 69.54$ can be seen distinctly in Fig. 2(d-i). Quantitative phase analysis shows the presence of cubic $LiCoO_2$ (46%) and Co_3O_4 (54%). The characteristic peaks of Co_3O_4 are superimposed with those of cubic $LiCoO_2$ and are shown with square symbols [Fig. 2(c-ii)]. The absence of any CoO in this sample implies that upon heating to 300 °C, the high temperature stable CoO is converted to the low temperature stable form, Co_3O_4. The diffractogram for the sample C5 is shown in [Fig. 2(c-iii)]. The peaks show an increase in intensity and sharpness, indicating increased crystallinity. The diffractogram is marked by prominent changes in comparison to Fig. 2(c-ii). The peak at $2\theta = 37.54$ shows a decrease in intensity, and the peak at $2\theta = 19.08$ shows an increase. Also, the (220) peak at $2\theta = 31.42$ disappears and the peaks at $2\theta = 65.70$ and 69.80 show a splitting [Figs. 2(c-iii) and 2(d-ii)] characteristic of the rhombohedral $LiCoO_2$. The phase analysis results indicate the presence of both cubic and rhombohedral phases of $LiCoO_2$, the relative proportion being 15% and 85%, respectively. No oxide of cobalt is detected, suggesting complete conversion of Co_3O_4 to $LiCoO_2$ on heat-treating at 500 °C. These results are in conformity with the results of thermal analysis as shown in Fig. 1(b).

Figure 2(c-iv) shows the x-ray diffractogram for sample C8. The peaks are very sharp, suggesting a higher degree of crystallinity. All the peaks could be indexed as the rhombohedral phase of $LiCoO_2$. The peak (003) at $2\theta = 19.08$ now is the most intense peak, and the higher

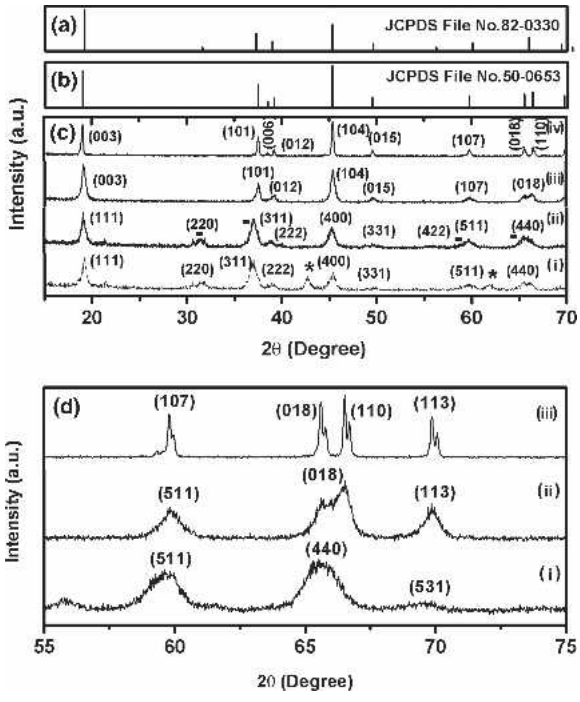

FIG. 2. Standard XRD lines for (a) cubic $LiCoO_2$ and (b) rhombohedral $LiCoO_2$. (c) X-ray diffractograms of $LiCoO_2$ nanocrystalline powders calcined at different temperatures: (i) as-synthesized, (ii) 300 °C, (iii) 500 °C, and (iv) 800 °C (* denotes the CoO phase and ▪ denotes the Co_3O_4 phase). (d) Slow-scanned x-ray diffractograms of nanocrystalline $LiCoO_2$ powders calcined at different temperatures: (i) 300 °C, (ii) 500 °C, and (iii) 800 °C.

angle peaks at $2\theta = 65.54$ (018) and 66.46 (110) are completely split [Figs. 2(c-iv) and 2(d-iii)], which is characteristic of rhombohedral $LiCoO_2$. Also, the peak at $2\theta = 69.82$ shows some splitting [Fig. 2(d-iii)]. The peaks (006) at $2\theta = 38.53$ and (012) at $2\theta = 39.19$ [Fig. 2(c-iv)] are well separated in C8 but exhibited an overlapped profile in the reflection patterns of C3, as observed in several other studies as well.[4,8,9,22,23] The prominent changes in the higher angle peaks were revealed by the slow-scanned x-ray diffractograms [Fig. 2(d)] of samples C3, C5, and C8 in the range $55° \leqslant 2\theta \leqslant 75°$, where the splitting of peaks at $2\theta = 65.6$, 66.52, and 69.88 can be clearly observed. A detailed phase analysis along with lattice parameters is summarized in Table I. To complement XRD data for phase determination of rhombohedral and cubic $LiCoO_2$, a FTIR study was carried out on sample C3 and C8 in the wave number range 2500–400 cm^{-1}, and the results are shown in Fig. 3. The spectra were analyzed in terms of localized vibrations of CoO_6 and LiO_6 moieties in the layered rhombohedral structure of $LiCoO_2$. The spectrum of C8 shows characteristic vibrational peaks for rhombohedral $LiCoO_2$ of space group $R\bar{3}m$ (C8) in the region of 600–400 cm^{-1} corresponding to the rock-salt band, broken into distinct peaks at 616 and 510 cm^{-1} closely resembling values found in the literature.[24–28] These vibrations are due to the stretching of Co–O bonds and bending of O–Co–O bonds in the CoO_6 octahedral moiety of rhombohedral $LiCoO_2$.[24,25] The vibrations due to the LiO_6 octahedral moiety occur in the region of 200 cm^{-1} and therefore could not be recorded due to instrumental limitations. The FTIR spectrum for the sample C3 was found to be different from that of rhombohedral $LiCoO_2$ (C8), showing the characteristic broad bands. It shows peaks at 450, 561, 668 cm^{-1} with a small shoulder at 867 cm^{-1}. The broad peaks found in the region of 1650–1200 cm^{-1} are due to residual organic moieties like the nitrate and carboxylate group. The sharp peak in the region of 2365 cm^{-1} found for both the samples (C3 and C8) is due to ambient CO_2. Appearance of more modes in the spectrum of C3 than those for C8 indicates a distortion in the rhombohedral structure and suggests a cubic spinel type of structure.[25] A small band in the region of ~450 cm^{-1} may be assigned to the disordered structure of the precursor in C3, which is completely absent in C8 with formation of a more ordered layered structure.[25]

Field emission scanning electron (FE-SEM) micrographs for both cubic (C3) and rhombohedral $LiCoO_2$ (C8) powders show an agglomerated nature of the particles (Fig. 4). The estimated powder grain sizes are ~60 nm for the cubic and ~100 nm for the rhombohedral phase. However, the respective crystallite sizes, as

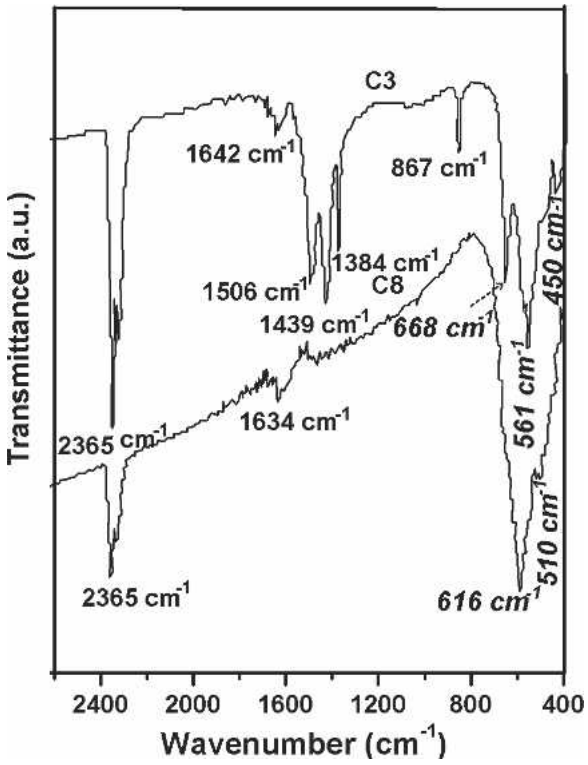

FIG. 3. FTIR spectra of nanocrystalline $LiCoO_2$ calcined at 300 °C (C3) and at 800 °C (C8).

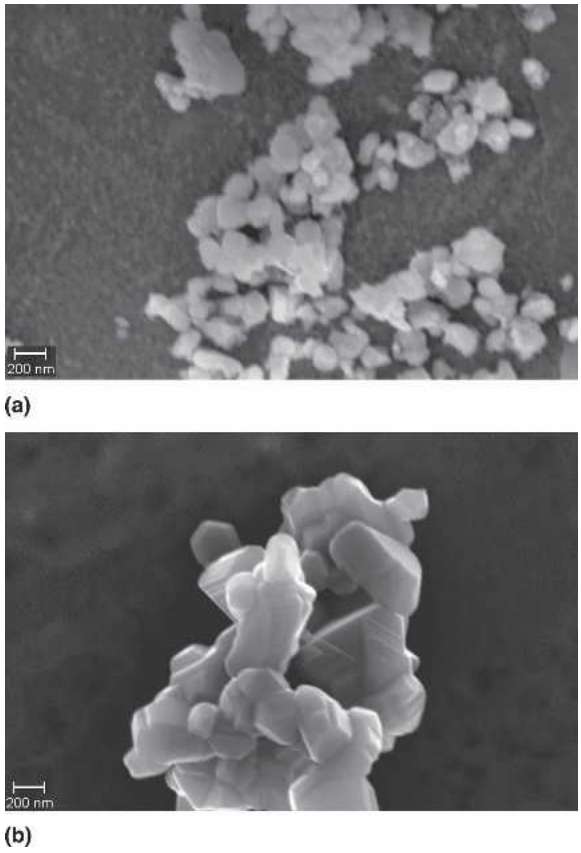

FIG. 4. FE-SEM micrographs of $LiCoO_2$ samples: (a) C3, calcined at 300 °C and (b) C8, calcined at 800 °C.

determined by XRD size analysis from the peak broadening, are found to be ~10 nm and ~51 nm (Table I).

Figure 5 shows the optical absorption spectra for samples C3, C5, and C8. The spectrum for Co_3O_4 is also included in the figure for comparison. The band gap values for the $LiCoO_2$ phase were estimated from the differential plot, δA versus wavelength, shown for sample C8 as a representative plot in the inset in Fig. 5. All the spectra are marked by three regions of absorption: I and II in the lower energy and III at the band edge. The spectra for both C3 and Co_3O_4 are very similar, and the estimated band gaps are ~1.43 and 1.47 eV, respectively. Two prominent shoulders are observed for all the samples in the lower energy region at ~0.65 and ~0.88 eV, similar to the observation of Kushida et al.,[5] originating probably due to some defect levels or from the electronic structure near the bottom of the conduction band. It is possible that some Co^{2+} ions on the tetrahedral sites might be responsible for this. It is interesting to note that although the cation distribution is different in the case of cubic $LiCoO_2$ and Co_3O_4,[15] there is a striking similarity between the optical spectra of sample C3 and Co_3O_4. With increase in the calcination temperature, the optical spectrum shows remarkable changes, and there is a notable blue shift in the band gap of $LiCoO_2$ calcined at 800 °C.[5] The band gap was found to be ~1.7 eV with shoulders of ~0.8 and ~0.65 eV. Variation in lithium content in the samples may strongly influence the band structure of $LiCoO_2$; however, from the ICP analyses the Li:Co ratio was found to be 1.02 for all the samples. Therefore, the observed blue shift in the band gap of C8 is not due to the variation in stoichiometry. As shown by XRD analysis, the phase present is 100% rhombohedral $LiCoO_2$, of space group $R\bar{3}m$. The octahedral ligand field of oxygen ions is strong enough to cause spin pairing in Co^{3+} ions to form a lower valence band comprising of completely filled t_{2g} orbitals and a conduction band of two empty e_g orbitals, and the d-d transition of electrons takes place between these two levels of Co.[5,14] As the crystallite size in the rhombohedral phase was found to be higher than that in the cubic phase (Table I), the observed blue shift cannot be explained on the basis of the size effect and must be related to changes in the electronic structure. On passing from higher symmetry (cubic) to lower symmetry (rhombohedral), the valence band now is composed of three completely filled t_{2g} orbitals and the conduction band is formed from two empty e_g orbitals of low spin Co in the octahedral ligand field of oxygen ions. Here, the splitting between the t_{2g} and e_g orbitals increases by a factor of 9/4 of that in the tetrahedral field of Co in the cubic lattice of $LiCoO_2$.[16] The band gap of ~1.7 eV found for sample C8 agrees well with the calculated band gap value of rhombohedral $LiCoO_2$ by Czyzyk et al.[14] Thus, the band gap of rhombohedral $LiCoO_2$ is about 0.3 eV higher than the cubic form.

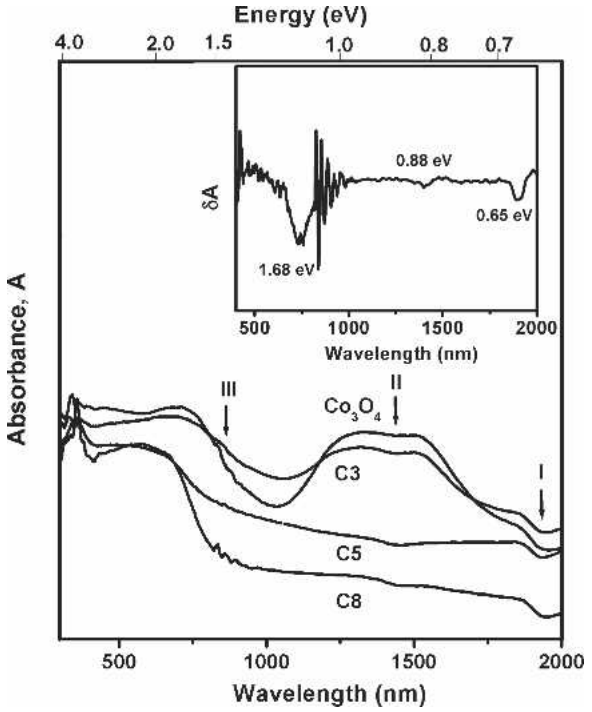

FIG. 5. UV-vis absorption spectra for nanocrystalline $LiCoO_2$ powders calcined at different temperatures at 300 °C (C3), 500 °C (C5), and 800 °C (C8). The spectrum for Co_3O_4 is also shown for comparison. The inset shows a differential absorbance plot (δA) versus wavelength for sample C8.

The open circuit voltage (OCV) of a lithium ion cell can be given by the relation[29]

$$V_{OC} = (\phi_C - \phi_A)/e_0 \quad , \qquad (1)$$

where ϕ_C and ϕ_A are the cathode and anode work functions respectively, and e_0 is the magnitude of an electric charge. As ϕ_C becomes larger, V_{OC} increases. The electronic band structure of the cathode has a large influence on the work function of the cathode. The band gap in $LiCoO_2$ is formed by the separation between the t_{2g} nonbonding levels and the e_g antibonding levels that are again formed by the π-overlap between d_{xy}, d_{xz}, and d_{yz} orbitals and oxygen 2p orbitals and by the σ-overlap between $d_{3z^2-r^2}$ And $d_{x^2-y^2}$ orbitals and oxygen 2p orbitals, respectively.[30] Both theoretical[13,14,16] and experimental works suggest that in cobalt oxide, the Fermi level resides within the t_{2g} band while in $LiCoO_2$, it is above the t_{2g} band, close to it. As Li is intercalated into the oxide, the electron is transferred to the t_{2g} levels lowering the Fermi energy and increasing the work function of the cathode, resulting in an increase in the intercalation voltage and increased OCV. Indeed, it has been observed experimentally that the electrochemical extraction of Li takes place at a constant voltage plateau at 3.6 V on open circuit for Li/cubic $LiCoO_2$ cell,[8] whereas for Li/rhombohedral Li_xCoO_2 cell, the open circuit voltage is 4.5 V for $x = 1.0$.[31]

In contrast to the present results, Kushida et al.[5] observed a large red shift (0.9 eV) in the band gap of HT-$LiCoO_2$ for thin films deposited on SiO_2 substrates. However, thin films have always been known to have a band gap higher than that of bulk material.

The optical spectra of C5 lie in the region intermediate to the spectra of C3 and C8 with a band gap similar to C8 (~1.7 eV). The investigated band gap suggests a rhombohedral crystal structure for the sample C5, which is further supported by the quantitative x-ray analysis in Table I that shows a dominant rhombohedral phase along with a minor cubic phase of $LiCoO_2$. An additional transition at energies greater than 3.3 eV is also observed for all the samples and may be attributed to Li 1*s* to O 2*p* or O 2*p* to Co 3*d* transitions.

IV. CONCLUSIONS

Nanocrystalline (10–50 nm) $LiCoO_2$ powder can be obtained by combustion synthesis. As-synthesized powder has a cubic crystal structure, which gradually transforms irreversibly into the rhombohedral form at temperatures greater than 500 °C. A drastic change in the *d-d* transition is observed between these two structural forms of $LiCoO_2$. The transition becomes sharper and the band gap is blue-shifted by about 0.3 eV when the material passes from the higher to the lower symmetry. These findings partly explain why the electrochemical performance of rhombohedral $LiCoO_2$ is better than that of the cubic form.

ACKNOWLEDGMENT

The authors wish to thank the Director of Central Glass and Ceramic Research Institute, Kolkata, for his kind permission to publish this paper.

REFERENCES

1. T. Nagaura and K. Tozawa: Lithium ion rechargeable battery. *Prog. Batt. Sol. Cells* **9,** 209 (1990).
2. P. Kalyani, R. Jagannathan, S. Gopukumar, and C-H. Lu: Luminescence in some lithiated transition metal oxide cathodes. *J. Power Sources* **109,** 301 (2002).
3. K. Mizushima, P.C. Jones, P.J. Wiseman, and J.B. Goodenough: Li_xCoO_2 ($0 < x < -1$): A new cathode material for batteries of high energy density. *Mater. Res. Bull.* **15,** 783 (1980).
4. R.J. Gummow, D.C. Liles, M.M. Thackeray, and W.I.F. David: A reinvestigation of the structures of lithium cobalt oxide with neutron diffraction data. *Mater. Res. Bull.* **28,** 1177 (1993).
5. K. Kushida and K. Kuriyama: Narrowing of the Co-3*d* band related to the order-disorder phase transition in $LiCoO_2$. *Solid State Commun.* **123,** 349 (2002).
6. E. Rossen, J.N. Reimers, and J.R. Dann: Synthesis and electrochemistry of spinel LT-$LiCoO_2$. *Solid State Ionics* **62,** 53 (1993).
7. S.G. Kang, S.Y. Kang, K.S. Ryn, and S.H. Chang: Electrochemical and structural properties of HT-$LiCoO_2$ and LT-$LiCoO_2$ prepared by the citrate sol-gel method. *Solid State Ionics* **120,** 155 (1999).
8. R.J. Gummow, M.M. Thakeray, W.I.F. David, and S. Hull: Structure and electrochemistry of lithium cobalt oxide synthesized at 400 °C. *Mater. Res. Bull.* **27,** 327 (1992).
9. Y.S. Horn, S.A. Hackney, A.J. Kahain, and M.M. Thackeray: Structural stability of $LiCoO_2$ at 400 °C. *J. Solid State Chem.* **168,** 60 (2002).
10. E.I. Santiago, A.V.C. Andrade, C.O. Paira-Santos, and L.O.S. Bulhoẽs: Structural and electrochemical properties of $LiCoO_2$ prepared by combustion synthesis. *Solid State Ionics* **158,** 91 (2003).
11. E. Antolini: $LiCoO_2$: Formation, structure, lithium and oxygen nonstoichiometry, electrochemical behavior and transport properties. *Solid State Ionics* **170,** 159 (2004).
12. K. Kushida and K. Kuriyama: Mott-type hopping conduction in the ordered and disordered phases of $LiCoO_2$. *Solid State Comm.* **129,** 525 (2004).
13. M.K. Aydinol, A.F. Kohan, and G. Ceder: Ab initio study of lithium intercalation in metal dichalcogenides. *Phys. Rev. B* **56,** 1354 (1997).
14. M.T. Czyzyk, R. Potze, and G.A. Sawatzky: Band-theory description of high-energy spectroscopy and the electronic structure of $LiCoO_2$. *Phys. Rev. B* **46,** 3729 (1992).
15. Y. Shao-Horn, S.A. Hackney, C.S. Johnson, A.J. Kahaian, and M.M. Thackeray: Structural features of low-temperature $LiCoO_2$ and acid-delithiated products. *J. Solid State Chem.* **140,** 116 (1998).
16. J. Van Elp, J.L. Wieland, H. Eskes, P. Kuiper, and G.A. Sawatzky: Electronic structure of CoO, Li-doped CoO and $LiCoO_2$. *Phys. Rev. B* **44,** 6090 (1991).
17. J.M. Rosolen and F. Decker: Photoelectrochemical behavior of $LiCoO_2$ membrane electrode. *J. Electroanal. Chem.* **501,** 253 (2001).
18. K. Kushida and K. Kuriyama: Optical absorption related to Co-3*d* bands in sol-gel grown $LiCoO_2$ films. *Solid State Commun.* **118,** 615 (2001).
19. R.N. Basu, F. Fietz, E. Wessel, H.P. Buchkremer, and D. Stöver: Microstructure and electrical conductivity of $LaNi_{0.6}Fe_{0.4}O_3$ prepared by combustion synthesis routes. *Mater. Res. Bull.* **39,** 1335 (2004).
20. K. Konstantinov, G.X. Wang, J. Yao, H.K. Liu, and S.X. Dou: Stoichiometry-controlled high-performance $LiCoO_2$ electrode materials prepared by a spray solution technique. *J. Power Sources* **119–121,** 195 (2003).
21. N.N. Greenwood and A. Earnshaw: *Chemistry of the Elements,* 1st ed. (Pergamon Press, Oxford, UK, 1984), pp. 1296–1297.
22. JCPDS Data File No. 00-043-1004, ICDD, PDF-2 Release 2003, US.
23. S. Choi and A. Manthiram: Synthesis and electrochemical properties of $LiCo_2O_4$ spinel cathodes. *J. Electrochem. Soc.* **149,** A162 (2002).
24. C. Julien: Local cationic environment in lithium nickel–cobalt oxides used as cathode materials for lithium batteries. *Solid State Ionics* **136–137,** 887 (2000).
25. C. Julien: Local structure and electrochemistry of lithium cobalt oxides and their doped compounds. *Solid State Ionics* **157,** 57 (2003).
26. G. Ceder and M.K. Aydinol: The electrochemical stability of lithium-metal oxides against metal reduction. *Solid State Ionics* **109,** 151 (1998).
27. S. Choi and A. Manthiram: Chemical synthesis and properties of spinel $Li_{1-x}Co_2O_{4-\delta}$. *J. Solid State Chem.* **164,** 332 (2002).
28. P. Kalyani, N. Kalaiselvi, and N. Muniyandi: A new solution combustion route to synthesize $LiCoO_2$ and $LiMn_2O_4$. *J. Power Sources* **111,** 232 (2002).
29. J.B. Goodenough: Design considerations. *Solid State Ionics* **69,** 184 (1994).
30. *Lithium Batteries Science and Technology,* edited by G-A. Nazri and G. Pistoia (Kluwer Academic Publishers, MA, 2004), p. 47.
31. E. Plitcha, S. Slane, M. Uchiyama, M. Salomon, D. Chua, W.B. Ebner, and H.W. Lin: An improved Li/Li_xCoO_2 rechargeable cell. *J. Electrochem. Soc.* **136,** 1865 (1989).